



HAL
open science

Falling-object protective structure for tractors in service: Prototype design and validation

L. Al-Bassit, N. Tricot, S. Sayegh

► To cite this version:

L. Al-Bassit, N. Tricot, S. Sayegh. Falling-object protective structure for tractors in service: Prototype design and validation. *Biosystems Engineering*, 2019, 185, pp.76-87. 10.1016/j.biosystemseng.2019.03.002 . hal-02609213

HAL Id: hal-02609213

<https://hal.inrae.fr/hal-02609213>

Submitted on 20 Jul 2022

HAL is a multi-disciplinary open access archive for the deposit and dissemination of scientific research documents, whether they are published or not. The documents may come from teaching and research institutions in France or abroad, or from public or private research centers.

L'archive ouverte pluridisciplinaire **HAL**, est destinée au dépôt et à la diffusion de documents scientifiques de niveau recherche, publiés ou non, émanant des établissements d'enseignement et de recherche français ou étrangers, des laboratoires publics ou privés.



Distributed under a Creative Commons Attribution - NonCommercial 4.0 International License

1 **Falling-Object Protective Structure for Tractors in Service: Prototype**

2 **Design and Validation**

3

4 Lama Al-Bassit, Nicolas Tricot, Simon Sayegh

5 Irstea – Centre de Clermont-Ferrand, 9 Avenue Blaise Pascal, CS 20085,63178 Aubière, France

6 lama.albassit@irstea.fr, nicolas.tricot@irstea.fr, simon.sayegh@irstea.fr

7

8 **Abstract**

9 A falling-object protective structure (FOPS) is a safety device fitted to self-propelled agricultural
10 vehicle that provides reasonable protection for the operator in the driving position against accidental
11 falling objects. To be certified, a FOPS undergoes a standardised full-scale destructive test to prove its
12 resistance to falling objects. This destructive test procedure is expensive and unsuitable for custom-
13 made FOPS manufactured individually. In the case of a tractor in service, for which manufacturers do
14 not offer a FOPS device, there is no certified method to evaluate the performance of a custom-
15 designed FOPS, other than this destructive procedure. The work described in this paper, funded by the
16 French Agriculture Ministry, proposes a design and a validation of a cantilever FOPS to equip tractors
17 that have two-post rear roll-over protective structures (ROPS). The main requirement of the custom-
18 designed FOPS is to meet the performance and protection level of certified structures. A design
19 approach with the goal of achieving optimal design was adopted. At each stage, design alternatives are
20 compared qualitatively and quantitatively, using numerical simulation, to assist decision making. A
21 validation method based on mathematical modelling and full-scale tests, according to standardised test
22 conditions, was adopted. This validation process made it possible to approve the design choices and to
23 determine the scope of validity of the proposed FOPS.

24

25 **Nomenclature**

26	$\mathbf{0}_{ij}$	Zero matrix of dimension i,j
27	$\mathbf{1}_i$	Identity matrix of dimension i
28	A_A	Section area of ROPS post
29	A_C	Section area of roof frame beam
30	b	Width of the roof plate
31	E	Young modulus of the roof plate
32	E_A	Young modulus of the rollbar
33	E_C	Young modulus of the roof frame
34	\mathbf{f}	Vector of equivalent loads applied to the structure
35	F	Concentrated load applied to the plate
36	g	Gravity acceleration
37	\mathbf{g}	Vector of gravity acceleration expressed in the absolute coordinate system
38	h	Thickness of the roof plate
39	I_{zA}	Area moment of inertia about the z -axis of the ROPS post's cross-section
40	I_{zC}	Area moment of inertia about the z -axis of the roof frame's cross-section
41	k or $k(\zeta,\eta)$	Stiffness of the plate
42	\mathbf{K}	Stiffness matrix of the structure
43	l	Length of the plate
44	L_A	Height of the ROPS post

45	L_B	Horizontal distance from the ROPS top to the impact point
46	L_C	Length of the roof
47	l_{fa}	Length of the ROPS post in contact with the attachment bracket
48	l_{fb}	Length of the roof frame in contact with the attachment bracket
49	M	Mass of the falling object
50	m_f	Mass of the attachment bracket
51	p	Distributed load depicting the weight of the roof
52	\mathbf{q}	Generalised coordinates: $\mathbf{q}=[u_{xA} \ u_{yA} \ \varphi_{zA} \ u_{xB} \ u_{yB} \ \varphi_{zB}]^T$
53	\mathbf{q}_0	Generalised coordinates at static equilibrium: $\mathbf{q}_0=[u_{xA0} \ u_{yA0} \ \varphi_{zA0} \ u_{xB0} \ u_{yB0}$
54		$\varphi_{zB0}]^T$
55	\mathbf{q}_M	Generalised coordinates at the maximum displacement: $\mathbf{q}_M=[u_{xAM} \ u_{yAM} \ \varphi_{zAM}$
56		$u_{xBM} \ u_{yBM} \ \varphi_{zBM}]^T$
57	T	Kinetic energy at impact
58	U	Elastic strain energy
59	$u_{x(P)}$	Displacement along x-axis at point P
60	$u_{y(P)}$	Displacement along y-axis at point P
61	V	Potential energy associated with applied loads
62	w	Vertical displacement at point \mathbf{p} of load application
63	w_M	Maximum vertical displacement during impact
64	(ζ, η)	Coordinate of point \mathbf{p} of load application

65	θ	Angle of inclination of ROPS posts with respect to the vertical
66	Π	Total potential energy
67	ν	Poisson ratio of the plate
68	$\varphi_{z(P)}$	Rotation around z-axis of the beam section at P

69

70 **1. Introduction**

71 Falling-object protective structures (FOPS) and roll-over protective structures (ROPS) are safety
72 devices fitted to self-propelled agricultural, forestry, mining and construction vehicles. According to
73 the ISO 27850:2013 international standard, a FOPS is an “assembly providing reasonable overhead
74 protection to an operator in driving position from falling objects” and a ROPS is a “framework (safety
75 cab or frame) protecting operators of agricultural and forestry tractors that avoids or limits risk to the
76 operator resulting from accidental overturning during normal operation.”

77

78 **1.1. Falling-object protective structure regulation**

79 The protective structure or cab of a newly designed agricultural tractor requires proof of compliance
80 before being proposed on the market (Regulation EU No. 167/2013). A protective structure could be
81 certified as ROPS only or as ROPS and FOPS. To be FOPS-certified, the structure undergoes a
82 standardised destructive test, according to code 10 of the Organisation for Economic Co-operation and
83 Development (OECD), (OECD, 2017), to prove its resistance to falling objects. This test consists of
84 analysing the impact between a falling metallic sphere weighing 45 kg and the structure. At the
85 moment of impact, the energy of the falling sphere must reach 1365 J.

86 For tractors in service, regulations related to work equipment are applied. According to European
87 directive 2009/104/EC, work equipment presenting a risk due to falling objects must be fitted with

88 appropriate safety devices corresponding to this risk. According to the same directive, employers shall
89 take the measures necessary to ensure that the work equipment made available to workers is safe and
90 suitable for the work to be carried out. Therefore, the farmer is compelled by the safety regulations to
91 have FOPS on tractors used by farm employees if the tasks performed on the farm involve a risk of
92 falling objects.

93 If there is a risk of falling objects, then having FOPS on agricultural tractors is mandatory. When this
94 is the case, in-service tractors not equipped with FOPS by the manufacturer, or tractors for which a
95 FOPS device is no longer proposed, have no non-destructive evaluation method proving the resistance
96 of a custom-made structure to falling objects. For custom-made protective structures manufactured
97 individually, the standardised destructive test is expensive for farmers.

98

99 **1.2. Protective structure design and validation methods**

100 The problem related to designing and testing self-propelled vehicle protective structures has been
101 widely studied by researchers, in particular ROPSs. As for FOPSs, ROPSs need to be validated by a
102 standardised method. This method consists of a series of destructive tests, expensive and inappropriate
103 for structures manufactured in limited numbers. A great deal of research has been conducted to replace
104 the destructive tests with calculation methods or with numerical tests using finite element analysis
105 software.

106 Mangado, Arana, Jarén, Arazuri, and Arnal (2007) proposed a calculation method to design ROPSs
107 that are easy to build and adaptable to all tractor models lacking this kind of protective structure. With
108 the same objective, Harris (2008) developed a cost-effective ROPS (CROPS) with a prediction method
109 to evaluate performance characteristics of these ROPS. Ayers, Khorsandi, John, and Whitaker (2016)
110 proposed a computer-based program to provide a quick ROPS design, based on the standardised test.
111 Other studies and software were developed by research institutions in France (Irstea, 2004) and Italy
112 (INAIL, 2014) with the aim of offering methods for designing and implementing ROPSs for tractors in
113 service built without commercial ROPSs.

114 Alfaro, Arana, Arazuri, and Jarén (2010) conducted tests using the finite element method to assess the
115 safety provided by a ROPS standardised test. They concluded that finite element analysis can be used
116 to design safer ROPSs. Based on numerical simulation, Kumar, Rudresh, and Maruthi (2014) and
117 Kumar et al. (2015) presented a case study of designing a safe tractor cab. Fabbri and Ward (2002)
118 proposed and evaluated a finite element model for ROPS design. Khorsandi, Ayers, and Truster
119 (2017) proposed a non-linear finite element model to predict the behaviour of a ROPS under a
120 simulated standardised test.

121 In fields other than the agriculture, Karlinski, Rusinski, and Smolnicki (2008), Karlinski, Ptak, and
122 Działak (2013) and Derlukiewicz, Karlinski, and Iuk (2010) developed approaches, based on finite
123 element analysis, for mining vehicle protective structures, which led to the possibility of using
124 numerical simulation to design protective structures. Aiming to provide information helping in the
125 design and evaluation of ROPSs without a systematic destructive test, Clark, Thambiratnam, and
126 Perera (2006), Thambiratnam, Clark and Perera (2009) and Perera, Thambiratnam and Clark (2011)
127 conducted experimental and numerical dynamic impact analysis on a construction machine ROPS.
128 They confirmed that dynamic simulation techniques are reliable tools for enhancing the safety of
129 protective structures. Based on a systematic comparison of protective structure virtual tests and real
130 tests, Tokarczyk (2013) deduced an acceptable error to consider if the virtual test is used for
131 certification. Kim & Reid (2001) were interested in improving, simplifying and speeding up ROPS
132 finite element analysis by implementing a new element in finite element code to better model thin-
133 walled rectangular tubes.

134 It is notable that methods for designing and validating FOPS designs have been poorly studied by
135 researchers. Unlike the ROPS standardised test, which is based on a series of quasi-static loading, the
136 FOPS test is based on dynamic impact, and therefore the alternative methods based on static finite
137 element simulations proposed for ROPS cannot be used for FOPS.

138

139 **1.3. Objective**

140 The objective of the work described in this paper was to design a FOPS that is easy to reproduce and
141 to manufacture using generic parts and tools, for in-service tractors built without this kind of
142 protective structure. The focus here is on agriculture tractors that are equipped, or can be equipped,
143 with a two-post rear ROPS such as those proposed by Irstea software (Irstea, 2004). The FOPS to be
144 designed must meet the performance and the protection level of these of certified structures.

145

146 **2. Materials and methods**

147 To design a FOPS to be fitted on tractors with two-post rear ROPSs, the design requirements are
148 identified and the design alternatives at each stage are listed and compared to obtain optimised
149 solutions. The performance of the design selected is evaluated and the structure obtained is validated
150 by full-scale drop tests.

151

152 **2.1. Design approach**

153 Irstea software (Irstea, 2004), which is based on a calculation method, proposes a two-post rear ROPS
154 design for tractors without this protection. This ROPS is a frame constituted of welded steel
155 rectangular tubes (Fig. 1). If the tractor overturns the frame comes into contact with the ground and
156 helps support the tractor. This ensures a space for a clearance zone around the tractor's driver. The
157 dimensions of this clearance zone are specified in OECD code 4 (OECD, 2017).

158

159 **2.1.1. Design requirements**

160 The principal functional requirement of the structure to be designed is to protect the user from falling
161 objects, in other words, it should have a performance allowing it to successfully pass the standardised
162 test delineated in code 10 (OECD, 2017). This means that the structure must completely cover and
163 overlap the vertical projection of the clearance zone surrounding the operator, which is specified in

164 OECD (2017) code 4, and the clearance zone must not be penetrated by any part of the FOPS, nor by
165 the falling object during the impact. The existing two-post ROPS must not be modified at all. The
166 structure designed could be attached to the existing ROPS, but it must not modify its mechanical
167 properties, i.e. no welding to or drilling through the certified ROPS. The custom-designed structure
168 must not alter the operating space or the access to the driving position.

169

170 2.1.2. Evaluation of design alternatives

171 The architecture adopted for the proposed FOPS is a cantilever clamped on the two-post ROPS. It has
172 three main components: a horizontal roof plate covering the vertical projection of the clearance zone, a
173 frame supporting the roof plate, and an attachment system fixing the frame to the ROPS. For each
174 component, several design solutions were initially proposed. The selection criteria were determined
175 and then solutions were evaluated and/or compared according to these criteria:

176 a) Roof plate selection

177 The criteria used to choose the roof plate were: material resistance to impact, low weight, ability to
178 protect from weather conditions, ability to ensure good upward visibility, price and availability for
179 purchase. Five plate types were selected at this stage: a full steel plate, a polycarbonate plate, a
180 perforated steel plate, a perforated steel plate assembled with a polycarbonate plate and a ribbed steel
181 plate.

182 The roof's length and width will vary depending on the tractor dimensions. The thickness of the roof
183 plates was selected at this stage. Dynamic finite element analysis using the ANSYS/LS-DYNA®
184 solver version 14.0 (ANSYS, Inc., Canonsburg, PA, USA) was carried out to compare the resistance of
185 plates with different thicknesses. In the first stage, a finite element model was calibrated based on the
186 result of a real test, which consisted of a full-scale impact test on a steel plate using standardised test
187 energy (Fig. 2). In the second stage, drop test simulations were carried out on steel and polycarbonate

188 plates of different thicknesses. This comparative study guided the selection of the plates to be used in
189 the full-scale drop tests during the validation process.

190 b) Roof frame

191 Frames formed of welded squared tubes were proposed and evaluated according to the selection
192 criteria. The main selection criteria were: easy to construct, light weight and ability to sustain the
193 impact test. The position of the impact point in the standardised test, according to OECD code 10, was
194 estimated for each solution. The impact point proximity to the tubes forming the frame was considered
195 as one of the stiffness indicators because, upon impact, it leads to a lower vertical displacement of the
196 roof plate. Figure 3 shows a simplification of the architectures studied. The frame selected is marked
197 (1); however, frame (5) is also considered an appropriate solution due to its special architecture; it
198 includes crossbars so it does not require an additional plate.

199 c) Attachment system

200 The main comparison criteria considered for the selection of the attachment system were: strength,
201 compactness and ease of manufacturing. The strength of the proposed solutions was evaluated by
202 performing static finite element analysis using the CATIA V5 software package (Dassault Systèmes,
203 Vélizy-Villacoublay, France) (Fig. 4). This study concluded with a selection of an attachment system
204 based on a closed-angle bracket made of welded steel sheets (Fig. 5) bolted to the ROPS and frame. A
205 second comparative simulation study was conducted to size the attachment system of the solution
206 selected (thickness of the steel sheets, main lengths, etc.). Bolt specifications of the attachment system
207 and their tightening torque were determined at this stage.

208 The architecture of the FOPS, resulting from the design phase, is shown in Fig. 5.

209

210 **2.2. FOPS performance evaluation and validation process**

211 Several dimensional parameters of the FOPS are determined during the design process (e.g. most of
212 attachment system dimensions, dimensions of the frame tube sections); the other dimensional

213 parameters, such as the roof frame and the plates' external dimensions, vary depending on the tractor
214 and its ROPS dimensions. The validation process consists of:

- 215 • Identifying, in the case of elastic deformation, the influence of dimensional parameters related to
216 the tractor and ROPS dimensions on FOPS resistance;
- 217 • Identifying the values of these parameters corresponding to the worst cases, i.e. cases where
218 displacements and/or stress in an elastically deformed structure are maximum;
- 219 • Carrying out full-scale drop tests on structures built according to dimensions corresponding to the
220 worst cases and studying their behaviour and resistance to impact.

221 The impact energy of the standardised test results in, as reported below, plastic deformation. In the
222 structures studied herein, it was assumed that, for a group of similar structures having only a few
223 dimensional differences, the structure with the highest displacement value at the impact point during
224 the elastic deformation would continue to have the highest displacement value during the elastic-
225 plastic deformation. Therefore, displacements that were measured on the structures tested during the
226 impact determined the maximum displacement values in the structures with the same architecture.

227

228 2.2.1. Mathematical model

229 The mathematical model is established to identify the dimensional parameters influencing the values
230 of the structure displacements during the impact under the assumption of elastic strain:

231 a) Roof plate mathematical model

232 According to plate theory, vertical displacement, w , of a point \mathbf{p} (ζ, η) of a simply supported plate of
233 dimensions $l \times b \times h$, when applying a perpendicular static load, F , at \mathbf{p} is given by the following
234 equation (Szilard, 2003):

$$235 \quad w(\zeta, \eta) = \frac{F}{k(\zeta, \eta)} \quad (1)$$

236 where

237
$$k(\zeta, \eta) = \frac{48(1-\nu^2)}{\pi^2 l b E h^3} \sum_{m=1}^{\infty} \sum_{n=1}^{\infty} \frac{\sin^2(m\pi\zeta/l) \sin^2(n\pi\eta/b)}{[(m^2/l^2)+(n^2/b^2)]^2} \quad (2)$$

238 Under the assumptions that, during an impact with a rigid sphere, strains in the plate remain in the
 239 elastic domain and there are no dissipative phenomena, the maximum displacement, w_M , at the impact
 240 point verifies the following relation (displacement due to plate mass is ignored here):

241
$$w_M = \frac{Mg}{k} + \sqrt{\left(\frac{Mg}{k}\right)^2 + 2\frac{T}{k}} \quad (3)$$

242 As a result, roof plate deflection w_M increases if length l and/or width b of the plate increases and it
 243 decreases when thickness, h , of the plate increases.

244 b) FOPS/ROPS skeleton mathematical model

245 In this mathematical model, ROPS and FOPS were taken into account. The attachment system was
 246 considered as a rigid part. The FOPS/ROPS structure was modelled as a 2D structure consisting of two
 247 beams connected by a rigid bracket (Fig. 6). The mass of the roof plate and frame was modelled by the
 248 linear load applied to the horizontal beam. The linear mass density of the ROPS was not taken into
 249 account in the model adopted. Point B was the vertical projection of the impact point.

250 The mathematical expression of total potential energy of the ROPS/FOPS skeleton, Π , can be written
 251 as follows:

252
$$\Pi = \frac{1}{2} \mathbf{q}^T \mathbf{K} \mathbf{q} - \mathbf{q}^T \mathbf{f} \quad (4)$$

253 \mathbf{q} is the generalised coordinates and gives displacements, along x and y , and rotations, around z , of
 254 beam sections A and B in the global coordinate frame: $\mathbf{q} = [u_{xA} \quad u_{yA} \quad \varphi_{zA} \quad u_{xB} \quad u_{yB} \quad \varphi_{zB}]^T$.

255 The mathematical expressions of \mathbf{K} and \mathbf{f} are given in Eq. (24) and Eq. (25).

256 In the case of an impact on the skeleton with a falling rigid object, at point B, the maximum
 257 displacements of the structure could be calculated under the assumptions of elastic strain from the
 258 following expression, where T is the kinetic energy at the impact and \mathbf{q}_0 is the displacement of
 259 structure in equilibrium state (Eq. (26)):

$$T = \frac{1}{2}(\mathbf{q}_M - \mathbf{q}_0)^T \mathbf{K}(\mathbf{q}_M - \mathbf{q}_0) + (\mathbf{q}_M - \mathbf{q}_0)^T \begin{bmatrix} \mathbf{0}_{3 \times 1} \\ Mg \end{bmatrix} \quad (5)$$

Impact energy, T , modifies all components of the generalised coordinates. To compare the roles of the tractor and roll-bar geometric parameters on these variations, two cases were studied: case 1) was based on the hypothesis that all impact energy is used to produce a vertical displacement at an impact point, so only the fifth component of $\mathbf{q}_M - \mathbf{q}_0$ is non-null; case 2) was based on the hypothesis that all impact energy is used to produce a rotation of the roof around \mathbf{z} on A, so only the third component of $\mathbf{q}_M - \mathbf{q}_0$ is non-null.

This study shows that vertical displacement at the impact point increases, essentially when the distance of the impact point, $(L_B - l_{fb})$, increases (Fig. 6). Rotation around \mathbf{z} at attachment point A increases when the distance of the impact point, $(L_B - l_{fb})$, and the ROPS length, $(L_A - l_{fa})$, increase; the area moment of inertia, I_{zA} , and the area A_A of the ROPS tube's cross-section decrease (Fig. 6). Stress at section E increases when length $(L_B - l_{fb})$ increases. At section A, stress increases when length L_B increases.

273

2.2.2. Full-scale tests

The purpose of the full-scale tests was to validate the design parameters chosen and to obtain the scope of validity of the designed structure. The scope of validity allows us to predict, depending on a tractor dimensions and its ROPS dimensions, whether or not the designed structure will pass the standardised drop test successfully. Energy at the impact for all the drop tests carried out is equal to the energy in OECD code 10 (1365 J). The proposed design was validated in two steps: validation of the FOPS roof, i.e. components covering the clearance zone (roof plate or crossbars), then validation of the ROPS/FOPS skeleton, i.e. the components ensuring load transfer from the impact location to the tractor chassis.

a) Tests on the FOPS roof

284 Twelve drop tests on structures composed of a fixed frame holding different types of plates or
285 crossbars were carried out. A draw-wire displacement sensor was used, when possible, to measure
286 displacement below the intended impact point. The disadvantageous conditions, which lead to the
287 highest vertical displacement at the impact point, were adopted. These conditions are related to roof
288 dimensions and impact point position. The largest roof on a tractor is estimated and selected, 1.8 m
289 long, 1 m wide, and the position of the impact point giving the greatest displacement of the plate or
290 crossbars is determined, the centre of the unsupported rectangle. The roofs tested were composed of a
291 frame supporting the following types of plates or crossbars:

- 292 • Structural steel S235JR sheet, 1.5 mm thick,
- 293 • Perforated mild steel sheets, type R20T28 DIN24041, 46.28% open area, 3 mm thick,
- 294 • Perforated mild steel sheets, type R20T28 DIN24041, open area 46.28%, 2 mm thick,
- 295 • Polycarbonate plate Makrolon ® GP, 8 mm thick,
- 296 • Polycarbonate plate Makrolon ® GP, 5 mm thick,
- 297 • Ribbed steel sheet, roofing sheet, 0.75mm thick,
- 298 • 5-mm polycarbonate plate Makrolon ® GP superimposed on a perforated mild steel plate 2 mm
299 thick, type R20T28 DIN24041, 46.28% open area and
- 300 • Structural steel S235 crossbars profiled in L 40 × 40 × 3 mm spaced 190 mm, 95 mm, 142 mm, 166
301 mm and 179 mm apart.

302 b) Tests on the structure's skeleton

303 The strength of the attachment system was checked through four full-scale impact tests. The
304 disadvantageous conditions which maximise mechanical stress in the attachment system during an
305 impact were studied. Two strategies were considered: 1) maximising energy transmitted to the
306 attachment system during impact by minimising the energy employed in deforming the roof and the
307 ROPS or 2) maximising the loads applied at the attachment system during impact.

308 Based on the mathematical model, the following were deduced and adopted in the different impact
309 tests: 1) to minimise strain energy of the roof plate, the plate thickness, h , was maximised and the
310 impact point was selected very close to the roof frame, i.e. η is almost zero; 2) to minimise the strain

311 energy of the roof frame, the length (L_B-l_{fb}) was minimised by placing the impact point very close to
312 the attachment system; 3) to minimise the strain energy of the ROPS, the height (L_A-l_{fb}) was
313 minimised; 4) to maximise the torque applied to the attachment system, the distance between the
314 impact point and the attachment system, (L_B-l_{fb}), was maximised and the mass of the roof was
315 increased by maximising the roof dimensions.

316 The previous points were considered through four impact tests. The structures tested had reduced-
317 height rollbar ROPS, a 2-mm-thick structural steel roof plate, maximised roof dimensions (1.8×1 m).
318 Two sections of ROPS tubes were used in the structures tested: (25 × 25 × 3 mm) and (100 × 50 × 3
319 mm), which gave two different depths for the prisms of the attachment systems. For each section two
320 impacts, on two different points of the roof, were carried out: the point nearest the attachment system
321 and the farthest point.

322 The behaviour of the ROPS/FOPS skeleton during impact was studied through three full-scale tests. In
323 these tests, the impact point was positioned in the middle of the plate's unsupported rectangle (Fig. 7).
324 The first impact test was carried out on a structure with the same dimensions as one of those used
325 previously (i.e., the reduced-height ROPS, the ROPS section measuring 100 × 50 × 3 mm, the roof
326 measuring 1.8 × 1 m). The objective of this test was to validate the roof frame design parameters and
327 to estimate the roof vertical displacement during the impact without taking into account ROPS
328 displacement. For the two other tests, the disadvantageous conditions, which lead to the highest
329 vertical displacement of the ROPS/FOPS skeleton during impact, were considered. These conditions
330 maximise $|u_{yBM} - u_{yB0}|$ and $|\varphi_{zAM} - \varphi_{zA0}|$. To estimate the extreme values of dimensional parameters L_A ,
331 L_B , A_A and I_{zA} , a sample of 12 in-service tractors was studied and ROPS/FOPS were dimensioned for
332 these tractors. From this study, the following values were found and used for the structures tested: the
333 highest ROPS posts were about 2 m, the largest ROPS was less than 0.82 m, the longest roof was less
334 than 1.2 m, the smallest ROPS tube section was 80 × 50 × 3 mm and the average tube section was 100
335 × 40 × 4 mm (the second moment of area about the z-axis is considered to obtain the average cross-
336 section). Two ROPS/FOPS structures were built respecting these extreme values. ROPS tube section
337 of one of these structures was 80 × 50 × 3 mm and of the other was 100 × 40 × 4 mm. Structural steel

338 S235 was used for rollbars and frame tubes, and for the roof plate, the frame tube dimensions were 40
339 $\times 40 \times 2$ mm, the roof plate thickness was 1.5 mm. For each test, four draw-wire sensors were used.
340 Two sensors were attached to the farthest corners of the roof to measure the maximum vertical
341 displacement of the structure during impact and the other two sensors were attached to the highest
342 corners of the ROPS to measure the rollbar horizontal displacement.

343

344 **3. Results and discussion**

345

346 **3.1. Full-scale test results**

347 The results obtained and the decisions made based on full-scale tests are presented below.

348

349 3.1.1. Roof test results

350 Drop tests on different types of plates and crossbars (Fig. 8) showed that the most suitable roofs to
351 pass the standardised drop test, without breaking down or significant damage and with moderate
352 vertical displacement at the impact point, were those equipped by a 1.5-mm structural steel sheet, a 3-
353 mm perforated steel sheet type R20T28 DIN24041 with a 46.28% open area, a 5-mm polycarbonate
354 plate superimposed on a perforated steel sheet 2 mm thick and crossbars spaced 166 mm apart. During
355 these tests, the displacement measurement by the draw-wire displacement sensor was not always
356 successful. Based on a few successful measurements and by comparison, the maximum displacement
357 at the impact point for these four roofs was estimated to be < 120 mm.

358

359 3.1.2. Structure skeleton test results

360 The tests carried out on the attachment system showed that the attachment system designed was very
361 resistant to impact and its plastic deformation is negligible compared to other deformations of the roof
362 and ROPS. The triangular dimensions of the attachment system, materials, and the mounting used in
363 its construction, should be adopted to be used for all new FOPSs. The only dimension which will
364 change from one FOPS to another is the depth of the triangular prisms to fit different ROPS tube
365 dimensions.

366 The tests on the structure's skeleton showed the following:

367 • During impact, the horizontal displacement of the ROPS for the three structures tested remained in
368 the elastic domain. Its maximum value, observed on the structure with the smallest ROPS tube section
369 ($80 \times 50 \times 3$ mm), was roughly ± 37 mm (Fig. 9).

370 • During impact, roof frames underwent elastic-plastic deformation. After impact, the roof frames
371 had a permanent downward inclination (Fig. 10). For the three structures tested, this inclination angle
372 was less than 10.2° . Despite this result, the dimension of the frame tube section ($40 \times 40 \times 2$ mm) was
373 adopted for all new designed FOPS.

374 • Although the displacement sensors were not always effective for measuring the vertical
375 displacement during impact (wire breakage, rewinding acceleration slower than the structure
376 movement during shock, etc.), a maximum inclination angle during impact was estimated to be $< 18^\circ$.

377

378 3.1.3. Limits of the validity of the proposed FOPS

379 The proposed FOPS was designed to fit on tractors which have, or may have, two-post ROPS of a
380 specific family. These ROPS, which are proposed by Irstea software, are made of welded rectangular
381 steel tubes. ROPS posts could be tilted towards the tractor rear at an angle of 15° maximum.

382 To fit the designed FOPS on an in-service tractor, the following dimensions must be determined
383 according to the tractor and its ROPS dimensions:

384 • The length of the roof must cover the horizontal projection of the clearance zone,

- 385 • The width of the roof must be equal to the ROPS width,
- 386 • The depth of the prism of the attachment system must be equal to the width of the ROPS tube,
- 387 • The angle of the ROPS posts to the vertical determines the angles of the prism to obtain a
- 388 horizontal roof.

389 The limits of the validity of this FOPS design are derived from the choices made during the validation

390 procedure and from the test results. For a tractor to be eligible to be fitted with the proposed FOPS, the

391 following conditions must be verified:

- 392 • The tractor ROPS must have an area moment of inertia of its cross-section greater than the 80×50
- 393 $\times 3$ mm tube;
- 394 • The ROPS height must be less than 2 m;
- 395 • The ROPS total width must be less than 0.82 m;
- 396 • The length of the rectangle covering the vertical projection of the standardised clearance zone,
- 397 measured from the top of the ROPS, must be less than 1.2 m.

398 From this study it can be deduced that, if the above conditions are valid, a custom-designed FOPS

399 respecting the design parameters adopted and validated in this study (i.e. roof materials, roof plate

400 thicknesses, roof frame tube section, attachment system material, dimensions and mounting, etc.) will

401 undergo deformation during an impact test according to code 10, which verifies that:

- 402 • The vertical displacement of the roof plate at the impact point remains below 120 mm and
- 403 • The inclination of the roof with respect to the horizontal remains below 18° .

404 A FOPS following this design will pass the standardised drop test and will not penetrate the clearance

405 zone during impact, if the vertical projection of the line connecting the top of the ROPS to the front

406 part, capable of supporting the tractor when overturned (point M in Fig. 11), has an angle, γ , greater

407 than 18° . This line, according to rollbar design, is always outside and above the clearance zone.

408 **3.2. FOPS implementation guiding tool**

409 The custom-designed FOPS was implemented on a David Brown 850 tractor (Fig. 12). The
410 manufacturing steps and instructions related to manufacturing are described in a guide to be used by
411 farmers wishing to install the FOPS on their tractors. A computer tool was implemented to guide users
412 in dimensioning FOPS appropriate for their tractors. With this computer tool, the farmer needs to input
413 data related to the tractor and the existing ROPS to obtain drawings of the FOPS parts to produce.

414

415 **4. Conclusions**

416 Depending on the use of agriculture tractors, the safety regulations require the presence of FOPSs. For
417 tractors in service, there is no currently available method to evaluate the performance of a designed
418 structure other than the standardised destructive test. In this study FOPSs are proposed for tractors that
419 do not have this type of protection. The proposed structures are able to pass the standardised test
420 successfully. A design process and a verification process were conducted to ensure that the proposed
421 structure's performance is equivalent to the performance of certified structures. The design process
422 was based on the systematic choice of optimised design solutions. The validation process was based
423 on full-scale impact tests carried out on few structures fulfilling the most challenging conditions. The
424 test results provide the scope of validity for the proposed structure. Knowing the dimensions of a
425 tractor, and the type and dimensions of its ROPS, a computer tool can be used to determine whether a
426 secure FOPS can be recommended for this tractor. In this case, drafts can be produced to guide the
427 user through the manufacturing of the FOPS.

428 This study focused on tractors in service that have, or could have, two-post rear ROPSs designed using
429 the Irstea software (Irstea, 2004). In an upcoming study future perspectives will be explored
430 examining FOPS for all tractors in service that do not have this protective structure but especially
431 those having two-post rear ROPS with a different architecture. A computer tool to guide the sizing and
432 manufacturing of FOPS, for all tractors in use, will be finalised and proposed to farmers and owners of
433 agriculture tractors.

434

435 **Acknowledgments**

436 This study is funded by the French Ministry of Agriculture and Food. We thank the Irstea tractor
437 testing technical platform team for carrying out the full-scale tests under the direction of Mr. Thierry
438 Langle. We thank the student trainees who participated in this study, particularly, Mr. Emmanuel
439 Peigne for his contribution to the structure design. We also thank Mr. Thierry Langle for his valuable
440 advice and comments on this work.

441

442 **References**

- 443 **Alfaro, J. R., Arana, I., Arazuri, S., & Jarén, C.** (2010). Assessing the safety provided by SAE
444 J2194 Standard and Code 4 Standard code for testing ROPS, using finite element analysis. *Biosystems*
445 *Engineering*, 105, 189 – 197.
- 446 **Ayers, P. D., Khorsandi, F., John, Y., & Whitaker, G.** (2016). Development and evaluation of a
447 computer-based ROPS design program. *Journal for Agricultural Safety and Health*, 22(4), 247-260.
- 448 **Clark, B. J., Thambiratnam, D. P., & Perera, N. J.** (2006). Analytical and Experimental
449 Investigation of the Behaviour of a Rollover Protective Structure. *The Structural Engineer*, 84(1), 29-
450 34
- 451 **Derlukiewicz, D., Karlinski, J., & Iluk, A.** (2010). The Operator Protective Structures Testing for
452 Mining Machines. *Solid State Phenomena*, 165, 256-261
- 453 **Fabbri, A., & Ward, S.** (2002). Validation of a Finite Element Program for the Design of Roll-over
454 Protective Framed Structures (ROPS) for Agricultural Tractors. *Biosystems Engineering*, 81(3), 287 -
455 296

456 **Harris, J.** (2008), *Predicting the performance characteristics of assembled rollover protective*
457 *structure designs for tractors*. Phd dissertation, West Virginia University

458 **INAIL** (2014). *Guidelines: Installation of protection devices in the event of overturning of*
459 *agricultural or forestry tractors*, 4th revision. Retrieved (at 2018, January 10) from:
460 [https://www.inail.it/cs/internet/comunicazione/pubblicazioni/catalogo-generale/linstallazione-dei-](https://www.inail.it/cs/internet/comunicazione/pubblicazioni/catalogo-generale/linstallazione-dei-dispositivi-di-protezione.html)
461 [dispositivi-di-protezione.html](https://www.inail.it/cs/internet/comunicazione/pubblicazioni/catalogo-generale/linstallazione-dei-dispositivi-di-protezione.html)

462 **Irstea** (2004). Software for dimensioning rollbars for agricultural tractors. Retrieved (at 2018, January
463 10) from: <http://agriculture.gouv.fr/renversement-des-tracteurs>

464 **Karlinski, J., Rusinski, E., & Smolnicki, T.** (2008). Protective structures for construction and mining
465 machine operator. *Automation in Construction*,17, 232-244

466 **Karlinski, J., Ptak, M., & Działak, P.** (2013). Simulation tests of roll-over protection structure,
467 *Archives of civil and mechanical engineering*, 13(1),57-63.

468 **Khorsandi, F ., Ayers, P. D ., & Truster, T. J.** (2017). Developing and evaluating a finite element
469 model for predicting the two-posts rollover protective structure nonlinear behavior using SAE J2194
470 static test. *Biosystems Engineering*, 156, 96–107

471 **Kim, T. H. & Reid, S. R.** (2001). Multi-axial softening hinge model for tubular vehicle roll-over
472 protective structures. *International Journal of Mechanical Sciences*, 43, 2147-2170.

473 **Kumar, A., Rudresh, M., & Maruthi, B. H.** (2014). Design Optimization of CAB Roof for Rops and
474 Fops Failure. *International Journal Of Advances in Engineering and Management (IJAEM)* 1(1).

475 **Kumar, A., Mahajan, A., Prasanth, S., Darekar, S., Chellan, J., & Kumar, K.A.** (2015).
476 Agricultural Tractor Cabin Structure Design for Durability and Rollover Protective Structure Test.
477 SAE Technical Paper 2015-26-0163

478 **Mangado, J., Arana, J. I., Jarén, C., Arazuri, S. & Arnal, P.** (2007). Design Calculations on Roll-
479 over Protective Structures for Agricultural Tractors. *Biosystems Engineering*, 96(2), 181–191

480 **OECD** (2017).OECD Standard Codes for the Official Testing of Agricultural and Forestry Tractors.
481 Retrieved (at 2018, January 10) from: [http://www.oecd.org/tad/code/oecd-standard-codes-official-](http://www.oecd.org/tad/code/oecd-standard-codes-official-testing-agricultural-forestry-tractors.htm)
482 [testing-agricultural-forestry-tractors.htm](http://www.oecd.org/tad/code/oecd-standard-codes-official-testing-agricultural-forestry-tractors.htm)

483 **Perera, N., Thambiratnam, D., & Clark, B.** (2011). Safety enhancement of operator protection
484 systems on self-propelled mining equipment. *Australasian Mine Safety Journal*, 3(5), 68-74.

485 **Szilard, R.** (2004). *Theories and Applications of Plate Analysis*. JohnWiley & Sons, Hoboken, New
486 Jersey.

487 **Thambiratnam, D. P., Clark, B. J., & Perera, N. J.** (2009). Performance of a Rollover Protective
488 Structure for a Bulldozer. *Journal of Engineering Mechanics*, 135, 31-40.

489 **Tokarczyk, J.** (2013). Verification of Virtual Prototypes of Mining Machines for Technical Criterion.
490 In: H. Kim, S.I. Ao, & B. Rieger (Eds.) *IAENG Transactions on Engineering Technologies, Lecture*
491 *Notes in Electrical Engineering*, 170. Springer.

492

493 **Appendix**

494 **FOPS/ROPS skeleton mathematical model**

495 In this mathematical model, ROPS and FOPS skeletons are taken into account. The attachment system
496 is considered as a rigid body. The FOPS/ROPS structure is modelled as a 2D structure consisting of
497 two beams connected by a rigid bracket (Fig. 13). The FOPS plate is modelled by a linear force
498 applied to a horizontal frame. Point B is the vertical projection of the impact point. Only the part of the
499 frame attached to the rollbar, backward the impact point, is considered. The part removed is replaced
500 with a vertical force f and a torque t around the z -axis.

501 Let ρ_A be the area density of the roof plate and λ the linear mass density of the roof frame tube, then
502 the absolute scalar values of linear effort, p , of force f and of torque t , (Fig. 13), are:

503 $p=g(\lambda+b\rho_A/2)$ (6)

504 $f=g(L_C-L_B)b\rho_A/2$ (7)

505 $t=g(L_C-L_B)^2b\rho_A/4$ (8)

506 The linear mass density of the ROPS is not taken into account in the model adopted; its influence on
 507 the vertical displacement of point B is considered small compared to the influence of the other loads.

508 The total potential energy of the ROPS/FOPS skeleton, Π , is calculated as the sum of elastic strain
 509 energy, stored in the deformed beams, U , and the potential energy associated with the forces applied,
 510 V . The elastic strain energy of the beams OA and EB, which represent the ROPS and the FOPS,
 511 respectively, is:

512
$$U = \frac{1}{2} \mathbf{u}_A^T \mathbf{R}^T \mathbf{K}_A \mathbf{R} \mathbf{u}_A + \frac{1}{2} \begin{bmatrix} \mathbf{u}_E \\ \mathbf{u}_B \end{bmatrix}^T \mathbf{K}_C \begin{bmatrix} \mathbf{u}_E \\ \mathbf{u}_B \end{bmatrix}$$
 (9)

513 where:

514 • \mathbf{u}_A , \mathbf{u}_B and \mathbf{u}_E give the displacements and the rotations for the beam sections A, B and E in
 515 the global coordinate frame:

516
$$\mathbf{u}_A = \begin{bmatrix} u_{xA} & u_{yA} & \varphi_{zA} \end{bmatrix}^T$$
 (10)

517
$$\mathbf{u}_E = \begin{bmatrix} u_{xE} & u_{yE} & \varphi_{zE} \end{bmatrix}^T$$
 (11)

518
$$\mathbf{u}_B = \begin{bmatrix} u_{xB} & u_{yB} & \varphi_{zB} \end{bmatrix}^T$$
 (12)

519 • \mathbf{K}_A is the stiffness matrix of the beam OA given in its local coordinate frame:

520
$$\mathbf{K}_A = \frac{E_A}{(L_A-l_{fa})} \begin{bmatrix} A_A & 0 & 0 \\ 0 & \frac{12I_{zA}}{(L_A-l_{fa})^2} & \frac{-6I_{zA}}{(L_A-l_{fa})} \\ 0 & \frac{-6I_{zA}}{(L_A-l_{fa})} & 4I_{zA} \end{bmatrix}$$
 (13)

521 • The rotation matrix \mathbf{R} allows transforming the stiffness matrix of OA into the global
 522 coordinate frame:

$$523 \quad \mathbf{R} = \begin{bmatrix} -\sin \theta & \cos \theta & 0 \\ -\cos \theta & -\sin \theta & 0 \\ 0 & 0 & 1 \end{bmatrix} \quad (14)$$

524 • \mathbf{K}_C is the stiffness matrix of the beam EB given in the global coordinate frame:

$$525 \quad \mathbf{K}_C = \begin{bmatrix} \mathbf{K}_E & \mathbf{K}_{EB} \\ \mathbf{K}_{BE} & \mathbf{K}_B \end{bmatrix} \quad (15)$$

526 with $\mathbf{K}_{BE} = \mathbf{K}_{EB}^T$,

$$527 \quad \mathbf{K}_E = \frac{E_C}{(L_B - l_{fb})} \begin{bmatrix} A_C & 0 & 0 \\ 0 & \frac{12I_{zC}}{(L_B - l_{fb})^2} & \frac{6I_{zC}}{(L_B - l_{fb})} \\ 0 & \frac{6I_{zC}}{(L_B - l_{fb})} & 4I_{zC} \end{bmatrix}$$

$$528 \quad \mathbf{K}_B = \frac{E_C}{(L_B - l_{fb})} \begin{bmatrix} A_C & 0 & 0 \\ 0 & \frac{12I_{zC}}{(L_B - l_{fb})^2} & \frac{-6I_{zC}}{(L_B - l_{fb})} \\ 0 & \frac{-6I_{zC}}{(L_B - l_{fb})} & 4I_{zC} \end{bmatrix}$$

$$529 \quad \mathbf{K}_{EB} = \frac{E_C}{(L_B - l_{fb})} \begin{bmatrix} -A_C & 0 & 0 \\ 0 & \frac{-12I_{zC}}{(L_B - l_{fb})^2} & \frac{6I_{zC}}{(L_B - l_{fb})} \\ 0 & \frac{6I_{zC}}{(L_B - l_{fb})} & 2I_{zC} \end{bmatrix}.$$

530 The potential energy associated with the forces applied to the structure is calculated as the sum of the
 531 potential energy associated with the efforts applied at the horizontal beam and the gravitational energy
 532 of the attachment system:

$$533 \quad V = - \begin{bmatrix} \mathbf{u}_E \\ \mathbf{u}_B \end{bmatrix}^T \mathbf{p} - \mathbf{u}_B^T \mathbf{f}_B - m_f \mathbf{u}_G^T \mathbf{g} \quad (16)$$

534 where

$$535 \quad \mathbf{p} = -p \begin{bmatrix} 0 & \frac{(L_B - l_{fb})}{2} & \frac{(L_B - l_{fb})^2}{12} & 0 & \frac{(L_B - l_{fb})}{2} & -\frac{(L_B - l_{fb})^2}{12} \end{bmatrix}^T$$

536 $\mathbf{f}_B = [0 \quad -f \quad -t]^T$, $\mathbf{g} = [0 \quad -g \quad 0]^T$ and \mathbf{u}_G gives the displacements of the vertical projection of
537 the centre of mass, G, of the attachment system.

538 The points A, E and G belong to the same rigid body. Let \mathbf{d}_G be the vector GA of the non-deformed
539 structure, then:

$$540 \quad \begin{bmatrix} u_{xG} \\ u_{yG} \end{bmatrix} = \begin{bmatrix} u_{xA} \\ u_{yA} \end{bmatrix} + (\mathbf{1} - \mathbf{R}_{\varphi_A}) \mathbf{d}_G \quad (17)$$

541 For small deflections the previous relation could be written as:

$$542 \quad \begin{bmatrix} u_{xG} \\ u_{yG} \end{bmatrix} = \begin{bmatrix} u_{xA} \\ u_{yA} \end{bmatrix} + \varphi_{zA} \begin{bmatrix} 0 & 1 \\ -1 & 0 \end{bmatrix} \mathbf{d}_G \quad (18)$$

543 The vector \mathbf{u}_G could then be written as a function of \mathbf{u}_A :

$$544 \quad \mathbf{u}_G = \begin{bmatrix} 1 & 0 & d_{Gy} \\ 0 & 1 & -d_{Gx} \\ 0 & 0 & 1 \end{bmatrix} \mathbf{u}_A = \mathbf{D}_G \mathbf{u}_A \quad (19)$$

545 By applying the same reasoning on E, the following relation is obtained:

$$546 \quad \mathbf{u}_E = \begin{bmatrix} 1 & 0 & d_{Ey} \\ 0 & 1 & -d_{Ex} \\ 0 & 0 & 1 \end{bmatrix} \mathbf{u}_A = \mathbf{D}_E \mathbf{u}_A \quad (20)$$

547 The total potential energy, Π , of the structure is obtained by adding Eq. (9) and Eq. (16). Replacing \mathbf{u}_G
548 and \mathbf{u}_E by the relations of Eq. (19) and Eq. (20) gives:

$$549 \quad \Pi = \frac{1}{2} \mathbf{u}_A^T \mathbf{R}^T \mathbf{K}_A \mathbf{R} \mathbf{u}_A + \frac{1}{2} \begin{bmatrix} \mathbf{u}_A \\ \mathbf{u}_B \end{bmatrix}^T \begin{bmatrix} \mathbf{D}_E^T & \mathbf{0}_{3 \times 3} \\ \mathbf{0}_{3 \times 3} & \mathbf{1}_3 \end{bmatrix} \mathbf{K}_C \begin{bmatrix} \mathbf{D}_E & \mathbf{0}_{3 \times 3} \\ \mathbf{0}_{3 \times 3} & \mathbf{1}_3 \end{bmatrix} \begin{bmatrix} \mathbf{u}_A \\ \mathbf{u}_B \end{bmatrix} - \dots$$

550 ...
$$\begin{bmatrix} \mathbf{u}_A \\ \mathbf{u}_B \end{bmatrix}^T \begin{bmatrix} \mathbf{D}_E^T & \mathbf{0}_{3 \times 3} \\ \mathbf{0}_{3 \times 3} & \mathbf{1}_3 \end{bmatrix} \mathbf{p} - \mathbf{u}_B^T \mathbf{f}_B - m_f \mathbf{u}_A^T \mathbf{D}_G^T \mathbf{g} \quad (21)$$

551 Let the generalised coordinates, \mathbf{q} , be the vector

552
$$\mathbf{q} = \begin{bmatrix} \mathbf{u}_A \\ \mathbf{u}_B \end{bmatrix} \quad (22)$$

553 The total potential energy, Π , of the structure can be written as:

554
$$\Pi = \frac{1}{2} \mathbf{q}^T \mathbf{K} \mathbf{q} - \mathbf{q}^T \mathbf{f} \quad (23)$$

555 where

556
$$\mathbf{K} = \begin{bmatrix} \mathbf{R}^T \mathbf{K}_A \mathbf{R} & \mathbf{0}_{3 \times 3} \\ \mathbf{0}_{3 \times 3} & \mathbf{0}_{3 \times 3} \end{bmatrix} + \begin{bmatrix} \mathbf{D}_E & \mathbf{0}_{3 \times 3} \\ \mathbf{0}_{3 \times 3} & \mathbf{1}_3 \end{bmatrix}^T \mathbf{K}_C \begin{bmatrix} \mathbf{D}_E & \mathbf{0}_{3 \times 3} \\ \mathbf{0}_{3 \times 3} & \mathbf{1}_3 \end{bmatrix} \quad (24)$$

557 and
$$\mathbf{f} = \begin{bmatrix} \mathbf{D}_E^T & \mathbf{0}_{3 \times 3} \\ \mathbf{0}_{3 \times 3} & \mathbf{1}_3 \end{bmatrix} \mathbf{p} + \begin{bmatrix} m_f \mathbf{D}_G^T \mathbf{g} \\ \mathbf{f}_B \end{bmatrix} \quad (25)$$

558 The displacement of the structure in equilibrium state, given by \mathbf{q}_0 , is obtained when:

559
$$\frac{\partial \Pi}{\partial \mathbf{q}} = 0 \quad \text{and therefore}$$

560
$$\mathbf{K} \mathbf{q}_0 = \mathbf{f} \quad (26)$$

561 In the case of an impact on the skeleton with a falling object, at point B, the maximum displacements
 562 of the structure could be calculated under the following assumptions: the strain of the structure
 563 remains in the elastic domain during the impact; the falling object is a very rigid non-deformable
 564 body; the kinetic energy, T , of the falling object, at the moment of impact, is entirely converted into
 565 strain energy upon impact (i.e. there are no dissipative phenomena). The mechanical energy of the
 566 structure+falling object system is then conserved during impact. Mechanical energy at the instant of
 567 impact and at the instant of reaching the maximum displacement, \mathbf{q}_M , is expressed. It gives the
 568 following equation:

$$569 \quad T + \frac{1}{2} \mathbf{q}_0^T \mathbf{K} \mathbf{q}_0 - \mathbf{q}_0^T \left(\mathbf{f} - M \begin{bmatrix} \mathbf{0}_{3 \times 1} \\ \mathbf{g} \end{bmatrix} \right) = \frac{1}{2} \mathbf{q}_M^T \mathbf{K} \mathbf{q}_M - \mathbf{q}_M^T \left(\mathbf{f} - M \begin{bmatrix} \mathbf{0}_{3 \times 1} \\ \mathbf{g} \end{bmatrix} \right) \quad (27)$$

570 This could be written as:

$$571 \quad T = \frac{1}{2} (\mathbf{q}_M - \mathbf{q}_0)^T \mathbf{K} (\mathbf{q}_M - \mathbf{q}_0) + (\mathbf{q}_M - \mathbf{q}_0)^T \begin{bmatrix} \mathbf{0}_{3 \times 1} \\ M \mathbf{g} \end{bmatrix} \quad (28)$$

572

573

574 **Figure Captions**

575 Fig. 1- Tractor with a ROPS designed following the Irstea method (Irstea, 2004)

576 Fig. 2 - Structure and model used in the full-scale and simulation drop tests at the roof plate selection stage

577 Fig. 3 - Proposed frames with vertical projection of clearance zone (dashed line) and position of the impact point (circle)

578 Fig. 4 - Model used in simulation study for choosing attachment system architecture

579 Fig. 5 - FOPS architecture

580 Fig. 6 – (a) 2D modelling of FOPS/ROPS skeleton (segment OD is the ROPS post, DC is the FOPS frame, ADE is the
581 attachment bracket and B is the impact point), (b) vertical displacement at B (in m) as a function of the impact point position
582 (in m), (c) rotation at A (in degrees) as a function of the impact point position (in m), (d) rotation at A (in degrees) as a
583 function of ROPS height (in m), (e) rotation at A (in degrees) as a function of ROPS tube section area (in m²), (f) rotation at
584 A (in degrees) as a function of area moment of inertia of the ROPS tube's cross-section (in m⁴)

585 Fig. 7 - Structures, impact point and sensor wire attachment position for ROPS/FOPS skeleton tests

586 Fig. 8 - Drop tests on FOPS roof, roofs equipped with (a) 1.5-mm steel sheet, (b) ribbed steel plate, (c) 3-mm perforated steel
587 sheet, (d) 5-mm polycarbonate plate, (e) 5-mm polycarbonate plate superimposed on 2-mm perforated steel sheet, (f) 2-mm
588 perforated steel, (g) 8-mm polycarbonate plate, (h) crossbars spaced 190 mm apart and (i) crossbars spaced 179 mm apart

589 Fig. 9 - Horizontal displacement of ROPS during impact (ROPS tube section 80×50×3mm)

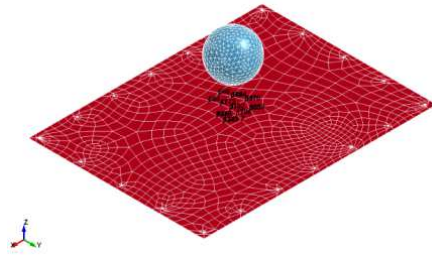
590 Fig. 10 - FOPS deformation after the impact

591 Fig. 11 - Schematisation of a tractor with its clearance zone (dotted line); M is the front point capable of supporting the
592 tractor when overturned

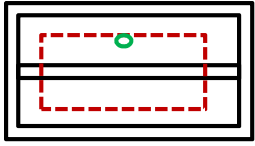
593 Fig. 12 - Tractor equipped with the custom-designed FOPS

594 Fig. 13 - Static loads applied to the structure studied and the clearance zone (grey area)

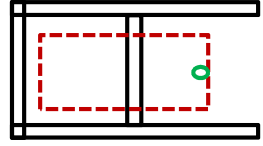




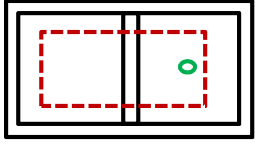
(1)



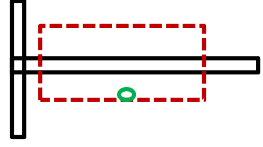
(2)



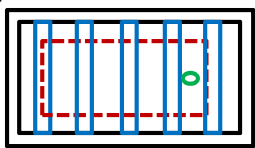
(2)



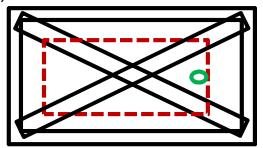
(3)

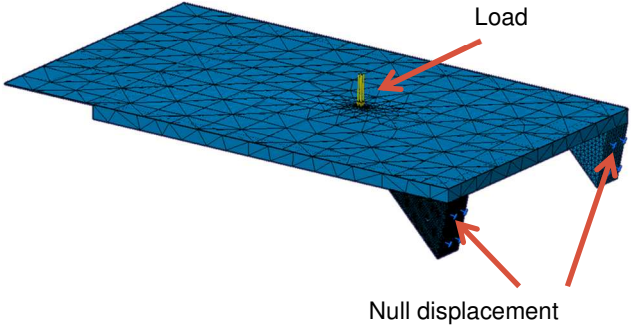


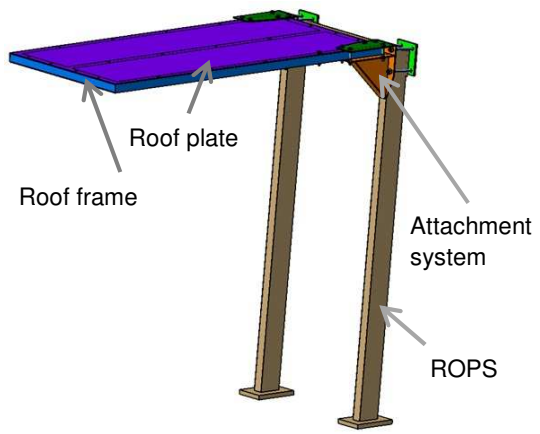
(5)

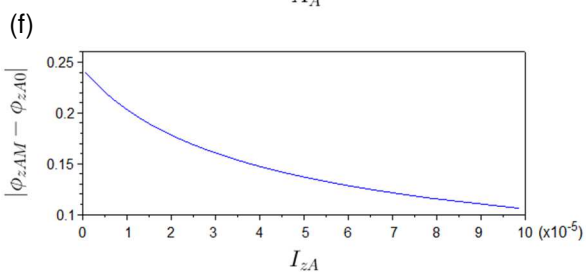
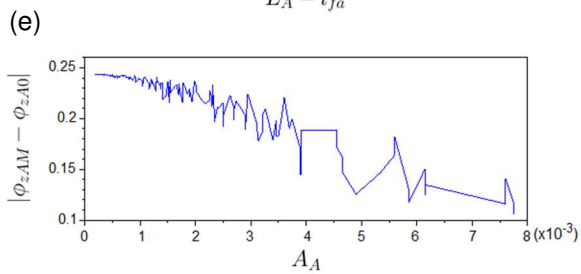
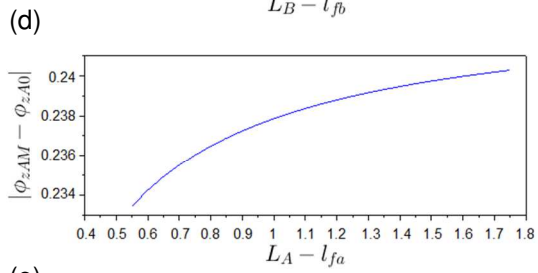
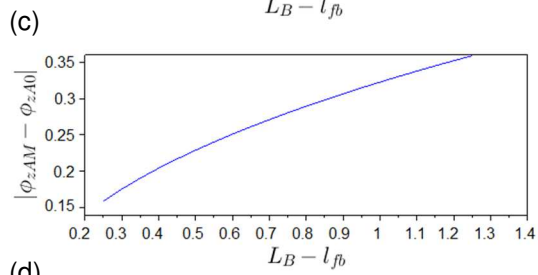
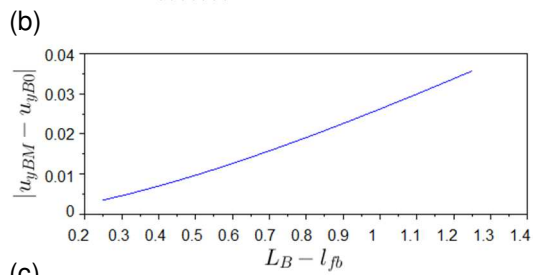
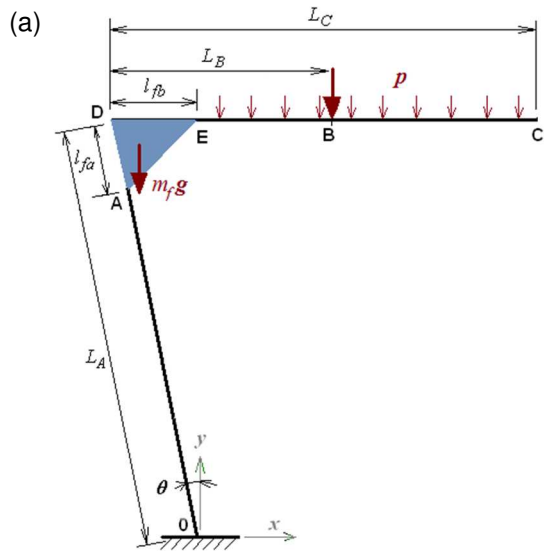


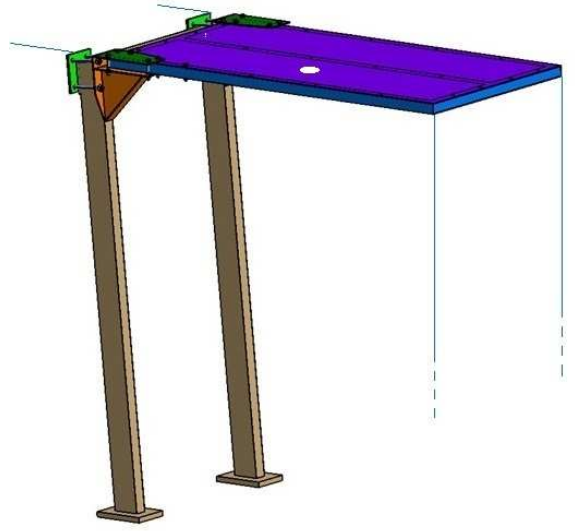
(6)



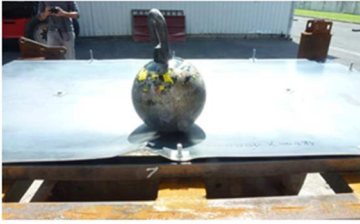








(a)



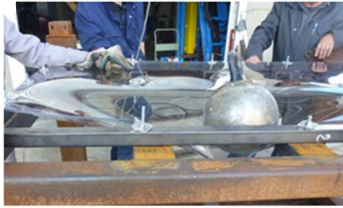
(b)



(c)



(d)



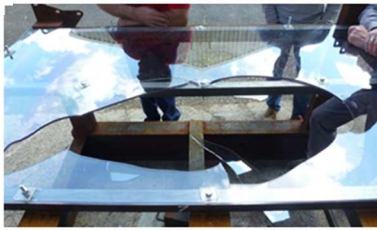
(e)



(f)



(g)



(h)



(i)



